Students Report: Polar vortex and sudden stratospheric warming 2020/21

Michel Michalkow
University of Leipzig
3281552
Students report
Course: dynamics of the middle atmosphere; Meteorology
16. February 2022

This report engages in the polar vortex and sudden stratospheric warmings (SSWs). As a case study the SSW at the north pole during 2020/21 was examined, with three different reanalysis models: ERA5, ICON-NWP and GEOS-FP. For the contributions of planetary and gravity waves, EP-Fluxes as well as Vertical Momentum Flux Convergence (VMFC) were evaluated. The results show large discrepancies between the resolved gravity wave forcings in the different models.

Keywords: stratosphere; polar vortex; sudden stratospheric warming; SSW20/21; EP-Flux; VMFC

1. Introduction

The polar vortices, both tropospheric and stratospheric, are playing and important role in earth climatology. The focus in this study is the stratospheric polar vortex, which, in case of sudden stratospheric warmings (SSWs) can have a significant influence on the tropospheric one and therefore alter the weather in the middle latitudes. Predicting these occurrences is of great interest for sub-seasonal to seasonal (S2S) weather and climate prediction efforts. Another aspect of interest are ozone dynamics: In a pronounced stratospheric polar vortex, ozone-reducing chemicals (e.g. NO_X) tend to accumulate, via the Brewer-Dobson Circulation, in the vortex, leading to an enhanced ozone destruction, in contrast to a broke-down vortex, where more mixing with mid-latitude air masses occurs.

1.1 polar vortex

Polar vortices are defined as strong westerly circumpolar wind bands, driven by the thermal wind balance from the temperature gradient due to the annual cycle of radiative equilibrium. While in the troposphere there are always two polar vortices present at the poles, in the stratosphere there is just one vortex at the current winter hemisphere, which is generally stronger then the tropospheric ones. At about 100 hPa in the winter hemisphere, one can observe a local minimum in westerly wind, constituting a distinction between tropospheric and stratospheric polar vortex.

1.2 vertical propagation of stationary waves

A first motivation, that wave propagation plays an important role in the dynamics of the middle atmosphere, is the fact that the observed temperature distribution in the mesopause differs greatly from what would be expected in the case of only radiative equilibrium. The sign of the temperature-gradient is even opposite [3]. This difference must be driven by eddy transport. A predominant contribution comes from vertically propagating quasi-stationary planetary waves [3]. From theoretical considerations one can derive the *Charney-Drazin criterion* for linear Rossby waves, and a zonal wind field independent of height and latitude, which is still - in a weaker sense - applicable for realistic situations. The criterion states that these waves can only vertically propagate in a mean zonal flow, which satisfies following condition:

$$0 < \overline{u} < \beta \Big[(k^2 + l^2) + f_0/(4N^2H^2) \Big]^{-1} \equiv U_c.$$

Here U_c could be called the *Rossby critical velocity*, and represents the upper bound. k and l are denoting the zonal and meridional wave numbers, N the *Brunt–Väisälä frequency*, f_0 the Coriolis parameter, β the meridional derivative of the Coriolis parameter and H the standard scale height.
The larger the amplitudes, the larger is the critical velocity. For the stratosphere the zonal wind speed overall increases with height, which means that larger-scale waves can propagate further upwards (in westerly winds).

1.3 sudden stratospheric warming

A sudden stratospheric warming is an event, where in the stratospheric polar vortex, temperatures are increasing suddenly and often rapidly, often 40 to 60 K in a week for the Arctic region. This increase is accompanied by a deceleration of the zonal wind. One can distinguish minor and major warmings: A major warming occurs when the zonal wind changes direction and the vortex therefore breaks down. On average Arctic stratospheric warmings occur 6 to 7 times per decade [6], while the Antarctic events are much less common. A main reason for this are the orographic differences of the hemispheres, as wave breaking in the middle atmosphere is the main driver of this warming. Especially wave-numbers of 1 and 2 play a major role. The break-down of these waves is associated with an convergence of the EP-Flux and leads to a deceleration of the zonal mean zonal wind. This, in combination with the *Charney-Drazin criterion*, leads to a feedback process: As the largest planetary waves may propagate up to the stratopause and also mesosphere, when they deposit their momentum, the reduced zonal wind allows now more smaller waves to propagate higher and also deposit their momentum. Depending on the available upward flux, this can proceed until the wind direction changes, which puts an end to this feedback at this certain layer. Radiative cooling then slowly reestablishes the cold polar temperatures, bringing back the normal westerlies. A SSW leads to a deformation of the vortex. Two common evolutions are either a splitting or a displacement. They are usually defined by the metrics *aspect ration* and *centroid latitude*. The weakening of the vortex slowly moves downwards and influences then the tropospheric vortex. This forms the link with the Northern Annular Mode/Arctic Oscillation (NAM/AO). The signal at the surface can follow several weeks after the initial event [7].

2. Data and methodology

To analyse the SSW in the year 2020/21, three different datasets were used:
1. The reanalysis data ERA5 [2], which provides 1-hourly datasets with a spatial resolution of 0.25°x0.25°, pressure levels up to 1 hPa and a sponge layer from 1 hPa upwards [1]. The sponge layer is an artificial mechanism, which "absorbs" waves in order to avoid artificial reflections induced by the numerical boundary conditions.
2. ICON-NWP data [8] with 0.25°x0.25° resolution (reshaped from the original triangular grid), pressure levels up to 1 hPa and a sponge layer from 44km ($\sim$ 2h Pa) upwards [5].
3. The analysis data GEOS-FP, also providing 6-hourly datasets with a spatial resolution of 0.3125°x0.25°, also with pressure levels up to 1 hPa, but an strong sponge layer from 0.04 hPa ($\sim$ 70 km) upwards [4].

For ERA5 data from 01.12.2020 to 01.02.2021, while for the other models data from 15.12.2020-07.01.2021 was downloaded. For every model 6-hourly datasets were used.

3. SSW 2020/21

One criterion for a major warming is the wind change at 10 hPa and 60°N (S). This is plotted for all three models in Fig. 1. The first occurrence of a wind direction change happened consistently on the fourth of January and is marked with a red line, which will be present as a marker in all following plots. The green line represents significant gravity-wave forcing at the same pressure level and latitude and will be introduced later, in the chapter about gravity waves, but is also present in all plots, as it will be handy for identifying the same time frame on different scales.

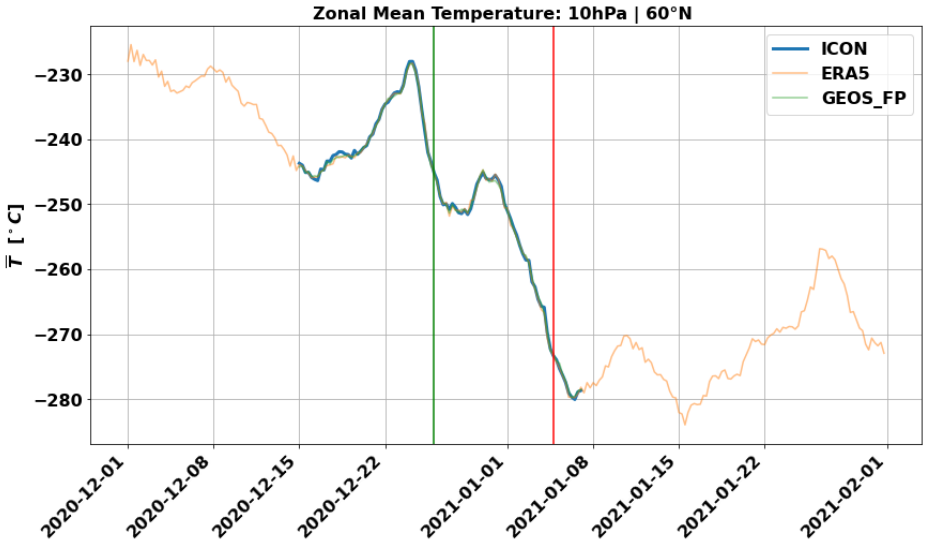

Figure 1. Zonal mean zonal wind for the 3 different models at 10 hPa and 60°N. The red line (SSW) denotes the date of the first major warming. The green line (GWF) denotes a Gravity Wave Forcing and is introduced in Fig. 7

.

Easterlies occurred first from 4 - 9 January and then again from 12 - 20 January of 2021. This is already longer than the mean duration of easterlies for all SSWs, which is 8 days [6]. A pressure resolved picture of the situation is given in Fig. 2 for ERA5. One can see reoccurring pulses weakening the westerlies, till a break-through at 1 hPa on the first of January. The following downward propagation is well visible for this break-through pulse.

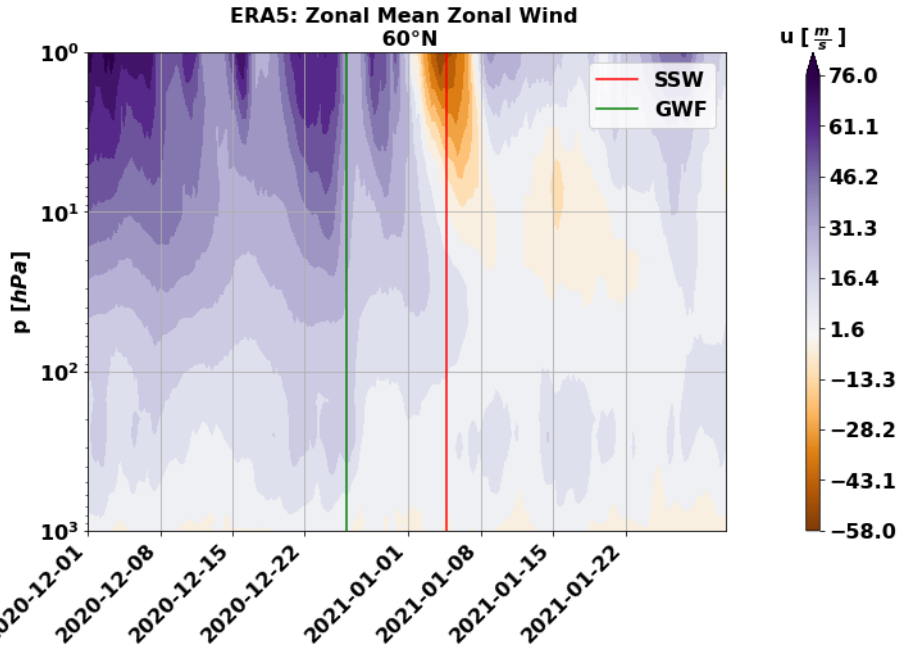

Figure 2. Zonal mean zonal wind for ERA5 at 60°N.

In Fig. 3 the same situation is shown for the temperature. Here one can see that the strongest warming already occurred before the wind direction changed. From theory it should be the other way around. The reason for this can maybe be better seen, looking at spatial distributions. An animated clip is available in the corresponding GitHub repository (see Appendix A), along with the code of the evaluation.

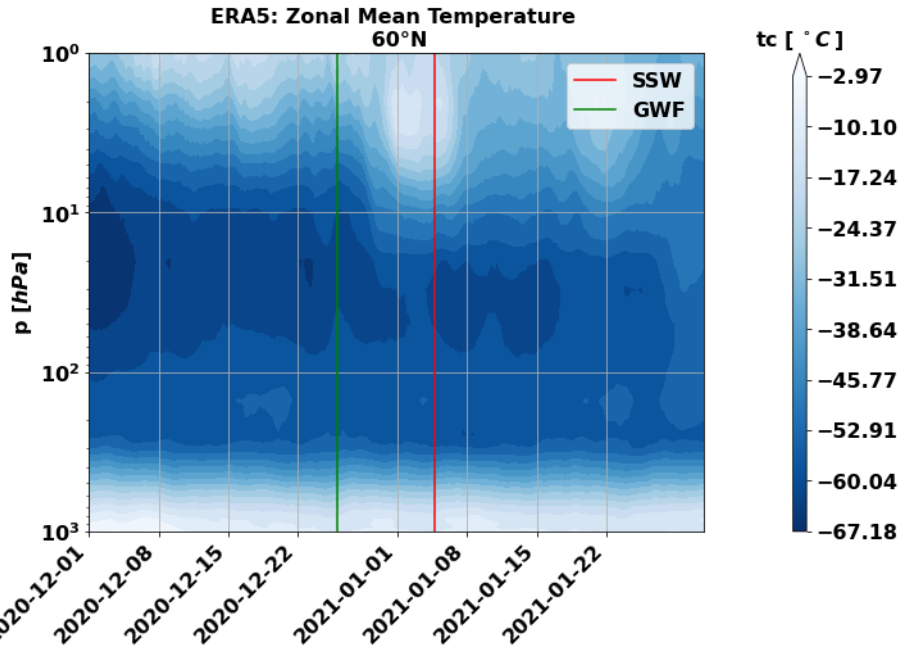

Figure 3. Zonal mean temperature for ERA5 at 60°N.

3.1 Eliassen–Palm flux

An interesting metric is the Eliassen–Palm flux, as the components can be used as proxies: The vertical component for the eddy heat flux and the meridional component for the momentum flux. The magnitude of the EP-divergence on the other hand is proportional to the eddy potential vorticity flux, which can be interpreted as an acceleration of the flow by waves for positive values and deceleration of the flow for negative values.

The vertical EP-Flux component is shown in Fig. 4 for two different height levels. Overall the heat flux is pointing upwards. At 10 hPa the sudden warming event is clearly visible. But also other minor warmings can be related to the temperature plot (Fig. 3). The heat flux of the GEOS-FP model is slightly - at the sudden warming even significant - weaker than that one of the other two models, although the GEOS-FP zonal mean temperature is consistent with the other models.

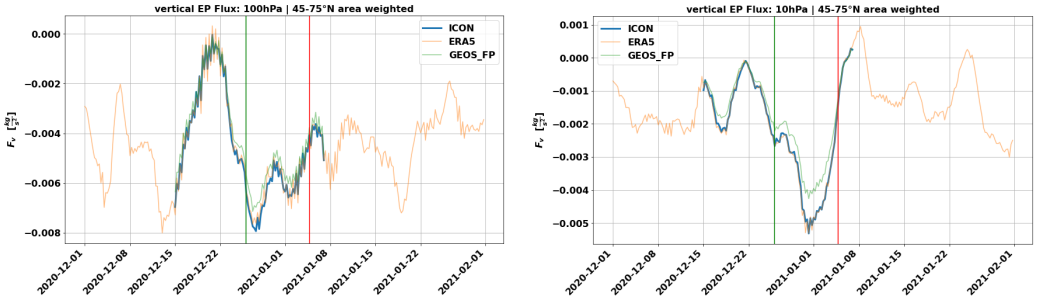

Figure 4. Vertical EP-Flux area averaged over 45-75°N at (a) 100 hPa and (b) 10 hPa for all three different models.

The same plots are shown for the meridional EP-Flux in Fig 5. Here the models are showing almost no differences. At 10 hPa one can compare this momentum flux proxy with the zonal wind in Fig. 2: An growth of this flux is accompanied with a deceleration of the westerlies and vice versa. The flow follows the momentum flux.

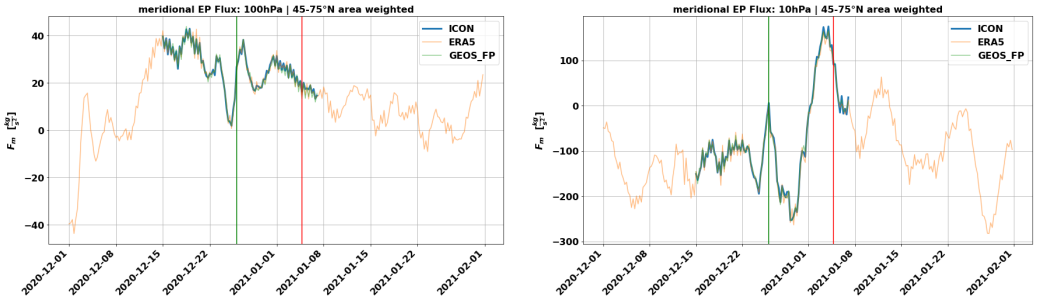

Figure 5. Meridional EP-Flux area averaged over 45-75°N at (a) 100 hPa and (b) 10 hPa for all three different models.

Finally a model comparison in pressure coordinates for the EP-Flux divergence is provided in Fig. 6. While the patterns seem to be consistent throughout the models, there are differences in the magnitudes.

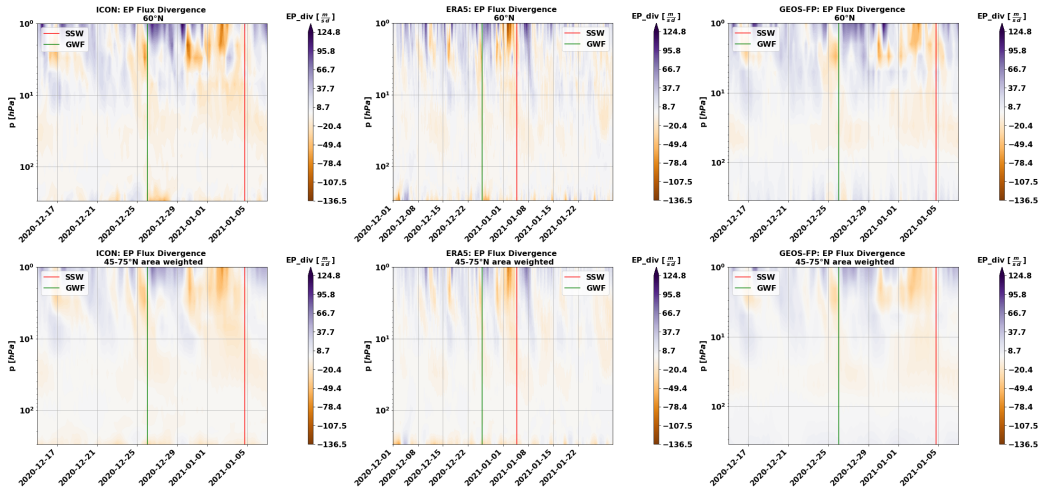

Figure 6. EP-Flux divergence for the three different models (columns) both at 60°N (upper row) and for the 45-75° area average (lower row).

3.2 Gravity Waves

Both planetary (PW) and gravity waves (GW) play an key role in middle atmospheric dynamics. GW are most important to consider in the mesosphere as they are the main driver of to pole-to-pole global circulation [1]. Besides PW also GW can play an important role in the stratospheric vortex breakdown. In models the vortex breakdown can be delayed up to several weeks [1], which can have a significant impact on seasonal forecasts. There are studies pointing to the inaccurate GW representation, as a reason for this model bias [1]. It is therefore interesting to investigate and compare the GW contributions, associated with the SSW, in different models. For this reason Gupta et al. [1] adapted a metric: The vertical momentum flux convergence (VMFC), as an estimation for the GW forcing only for zonal wavenumbers 21 and higher. This metric will be used here in the same sense.

At first, a look was taken at the usual 10 hPa and 60°N, to get an first impression. It is shown in Fig. 7. One sees a spike forcing around 25-26 December 2020 for both ERA5 and GEOS-FP. The spike for ICON-NWP is visible, but pretty weak. The extrema of the spike is used for defining the green line. Below in Fig. 8 is a model comparison, in pressure coordinates, which shows that this green line doesn't necessarily mark an important date. It is also clear, that the GW representation is quite diverse throughout the models. One commonality is that the strongest forcings take place near the ground or above (10-) 3 hPa, but magnitude and the actual structure are different. For ERA5 and GEOS-FP the area weighted average shows a band of active forcings above 3 hPa, which stays more or less constant throughout the time - for ERA5 even from the beginning of December. However, in GEOS-FP, this band shows often excrescences down to 10-100 hPa. In ICON-NWP this band is non existent; just a small forcing above 10 hPa, around the transitions to the new year, is visible. Notice that the colorbar is logarithmic; only in this Figure.

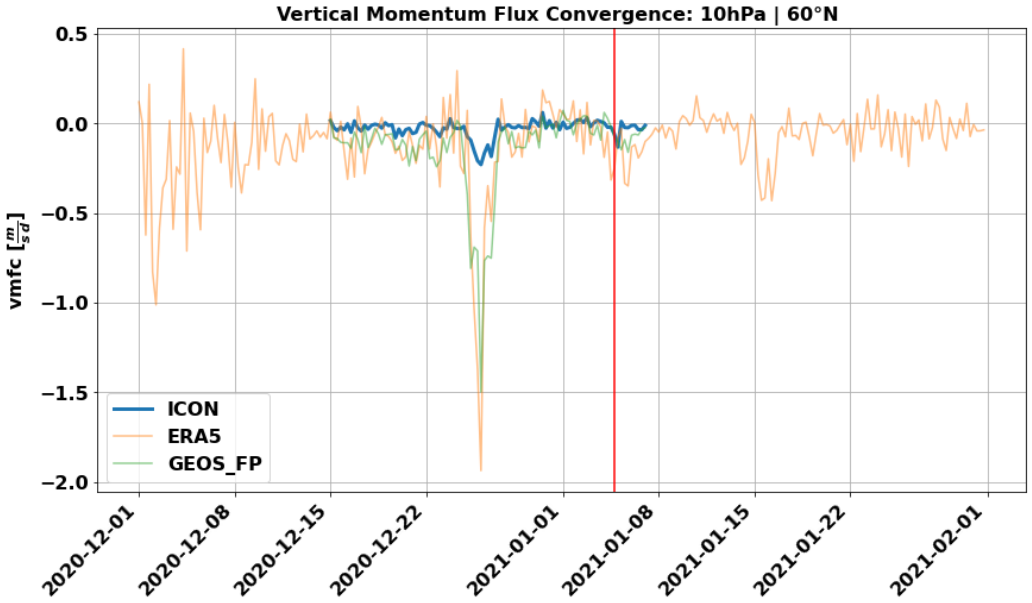

Figure 7. VMFC for the three different models at 60°N and 10 hPa

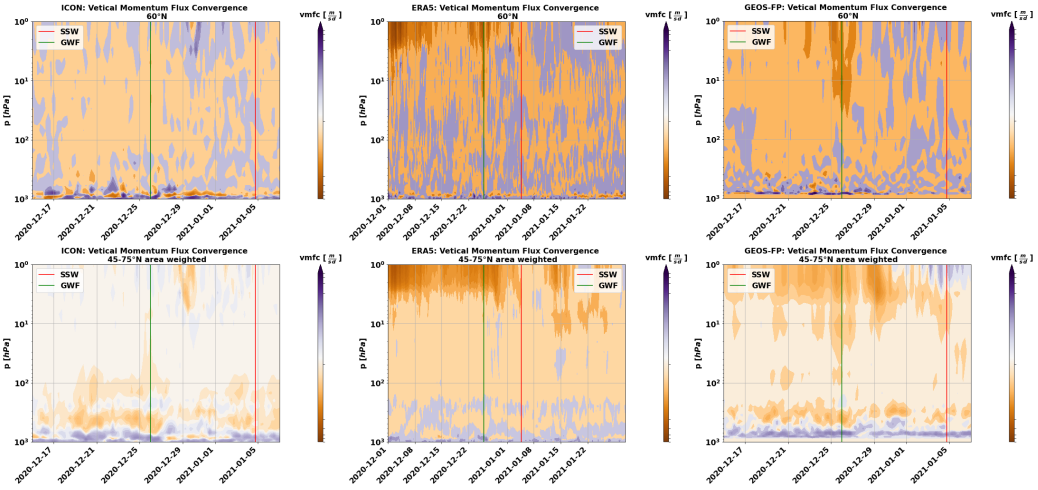

Figure 8. VMFC for the three different models (columns) both at 60°N (upper row) and for the 45-75° area average (lower row). The colorbars are all the same and logarithmic with a maximum (violet) of 6.58 $\frac{m}{sd}$ and a minimum (orange) of -8.31 $\frac{m}{sd}$.

4. Conclusion and outlook

In this work the forming and breaking of stratospheric polar vortices was examined. As a case study the major SSW of 2020/21 was analysed with three different models, ex-

ploring tools and possibilities to work with (re-)analysis datasets. Many aspects of the sudden warming event were consistently represented in the models. Some, like the vertical EP-Flux, showed little discrepancies, while the representation of gravity waves was pretty diverse. ERA5 and GEOS-FP suggest that the gravity waves forcing may be deposited evenly throughout the breakdown period. When comparing VMFC with EP-Flux divergence, VMFC seems almost negligible. Contrary Gupta et al. [1], state, that resolved GW provide around 25% of the net deceleration. As also stated by them, GW representation is very sensible to parametrizations and tuning, so it would make sense to look deeper into the model details, and also analyse different GW contributions, like orographic vs. non-orographic sources or the spectral components.

References

[1] Aman Gupta, Thomas Birner, Andreas Dörnbrack, and Inna Polichtchouk. **Importance of Gravity Wave Forcing for Springtime Southern Polar Vortex Breakdown as Revealed by ERA5**. *Geophysical Research Letters*, 48(10), 2021. doi:https://doi.org/10.1029/2021GL092762.

[2] Hans Hersbach, Bill Bell, Paul Berrisford, Shoji Hirahara, András Horányi, Joaquín Muñoz-Sabater, Julien Nicolas, Carole Peubey, Raluca Radu, Dinand Schepers, Adrian Simmons, Cornel Soci, Saleh Abdalla, Xavier Abellan, Gianpaolo Balsamo, Peter Bechtold, Gionata Biavati, Jean Bidlot, Massimo Bonavita, Giovanna De Chiara, Per Dahlgren, Dick Dee, Michail Diamantakis, Rossana Dragani, Johannes Flemming, Richard Forbes, Manuel Fuentes, Alan Geer, Leo Haimberger, Sean Healy, Robin J. Hogan, Elías Hólm, Marta Janisková, Sarah Keeley, Patrick Laloyaux, Philippe Lopez, Cristina Lupu, Gabor Radnoti, Patricia de Rosnay, Iryna Rozum, Freja Vamborg, Sebastien Villaume, and Jean-Noël Thépaut. **The ERA5 global reanalysis**. *Quarterly Journal of the Royal Meteorological Society*, 146(730):1999–2049, 2020. doi:https://doi.org/10.1002/qj.3803.

[3] James R. Holton and Gregory J. Hakim. ***An Introduction to Dynamic Meteorology. Fifth edition.*** Academic Press, Amsterdam, 2013.

[4] Masaru Kogure, Jia Yue, and Huixin Liu. **Gravity Wave Weakening During the 2019 Antarctic Stratospheric Sudden Warming**. *Geophysical Research Letters*, 48(8), 2021. doi:https://doi.org/10.1029/2021GL092537.

[5] Christopher G. Kruse, M. Joan Alexander, Lars Hoffmann, Annelize van Niekerk, Inna Polichtchouk, Julio T. Bacmeister, Laura Holt, Riwal Plougonven, Petr Šácha, Corwin Wright, Kaoru Sato, Ryosuke Shibuya, Sonja Gisinger, Manfred Ern, Catrin I. Meyer, and Olaf Stein. **Observed and Modeled Mountain Waves from the Surface to the Mesosphere Near the Drake Passage**. *Journal of the Atmospheric Sciences*, 2022. doi:10.1175/JAS-D-21-0252.1.

[6] Qian Lu, Jian Rao, Zhuoqi Liang, Dong Guo, Jingjia Luo, Siming Liu, Chun Wang, and Tian Wang. **The sudden stratospheric warming in January 2021**. *Environmental Research Letters*, 16(8):084029, jul 2021. doi:10.1088/1748-9326/ac12f4.

[7] James Overland, Richard Hall, Edward Hanna, Alexey Karpechko, Timo Vihma, Muyin Wang, and Xiangdong Zhang. **The Polar Vortex and Extreme Weather: The Beast from the East in Winter 2018**. *Atmosphere*, 11(6), 2020. doi:10.3390/atmos11060664.

[8] Günther Zängl, Daniel Reinert, Pilar Rípodas, and Michael Baldauf. **The ICON (ICOsahedral Non-hydrostatic) modelling framework of DWD and MPI-M: Description of the non-hydrostatic dynamical core**. *Quarterly Journal of the Royal Meteorological Society*, 141(687):563–579, 2015. doi:https://doi.org/10.1002/qj.2378.

Appendix

A. Code availability

The code of the evaluation, and also animations are available for reproducibility in this GitHub repository: https://github.com/VACILT/PV_characteristics_ICON-NWP/tree/main/student/Michel.